ELSEVIER

Thin Solid Films 420–421 (2002) 225–229

thin solid films

www.elsevier.com/locate/tsf

Growth of the large area horizontally-aligned carbon nanotubes by ECR-CVD

Chih Ming Hsu, Chao Hsun Lin, Hui Lin Chang, Cheng Tzu Kuo*

Department of Materials Science and Engineering, National Chiao Tung University, 1001 Ta-Hsueh Road, Hsinchu 300, Taiwan, ROC

Abstract

For potential applications of carbon nanotubes (CNTs) as connectors in microelectronic devices, the process to synthesize the large area horizontally-aligned CNTs on 100 mm (4 inch) Si wafers was developed, using electron cyclotron resonance chemical vapor deposition, with CH_4 and H_2 as the source gases and Co as the catalyst. The results show that vertical and horizontal CNTs can be obtained by manipulating the electric field applied on the substrate and flow direction of the gases. In the present deposition conditions, the horizontal CNTs show better field emission properties than vertical CNTs. This may be due to the blocking effect of catalysts at the tips and to the diminishment of the effective emission area from defects of vertical CNTs body.
© 2002 Elsevier Science B.V. All rights reserved.

Keywords: Chemical vapor deposition; Field emission; Carbon; Scanning electron microscopy

1. Introduction

In the past decade, carbon nanotubes (CNTs) have attracted intensive interest in nanotechnology due to their remarkable properties and applications, such as nanoelectronics [1–8], field emitters [9–13], hydrogen storage [14,15], scanning probe [16] and supercapacitors [17]. The CNTs have been synthesized by many methods, including arc discharge [18], laser ablation [19], microwave plasma chemical vapor deposition [20], thermal chemical vapor deposition (CVD) [21], etc. Most of these methods are designed to grow the vertically-oriented CNTs with respect to the substrate surface [22,23]. However, for microelectronic applications, it often demands to make horizontal interconnection between components. In these applications, horizontally-oriented CNTs have started to attract attention in both academic and industrial communities [24–28]. Other applications of the horizontally-oriented CNTs are to grow a single nanotube for study of single nanotube properties [28]. The purposes of this study were to investigate the main parameters that control the orientations of the CNTs or each single nanotube, and then to examine their properties and structures. In consideration of the advantages of high dissociation percentage of the precursor gases, high uniformity of plasma energy distribution, and possible large area film deposition, the electron cyclotron resonance chemical vapor deposition (ECR-CVD) method is adopted for this study.

2. Experimental

The horizontally-aligned CNTs were synthesized on 100 mm Si wafers by ECR-CVD method with CH_4/H_2 as the source gases. The Co catalyst for CNTs growth was applied on Si wafer by physical vapor deposition method, and followed by hydrogen plasma etching treatment for 15 min to become well-distributed nano-sized catalysts. To produce the horizontally-aligned CNTs, a Ti wafer about specimen size and ~2 mm in thickness was placed 1–2 mm on top of the specimen to guide the source gases to flow parallel to the specimen surface. A heater was provided in the specimen holder to maintain the deposition temperature. The deposition conditions for the CNTs growth were: microwave power 800 W, −200 V substrate bias, CH_4/H_2 ratio = 15/15 sccm, deposition times 5–15 min, pressure 0.25 Pa and deposition temperature 600 °C. For comparison, the CNTs grown by the guided flow for 5 and 15 min are called Samples A and B, respectively, and the sample

*Corresponding author. Tel.: +886-3-5731-949; fax: +886-3-5724-727.

E-mail address: ctkuo@cc.nctu.edu.tw (C.T. Kuo).

0040-6090/02/$ - see front matter © 2002 Elsevier Science B.V. All rights reserved.
PII: S0040-6090(02)00799-X

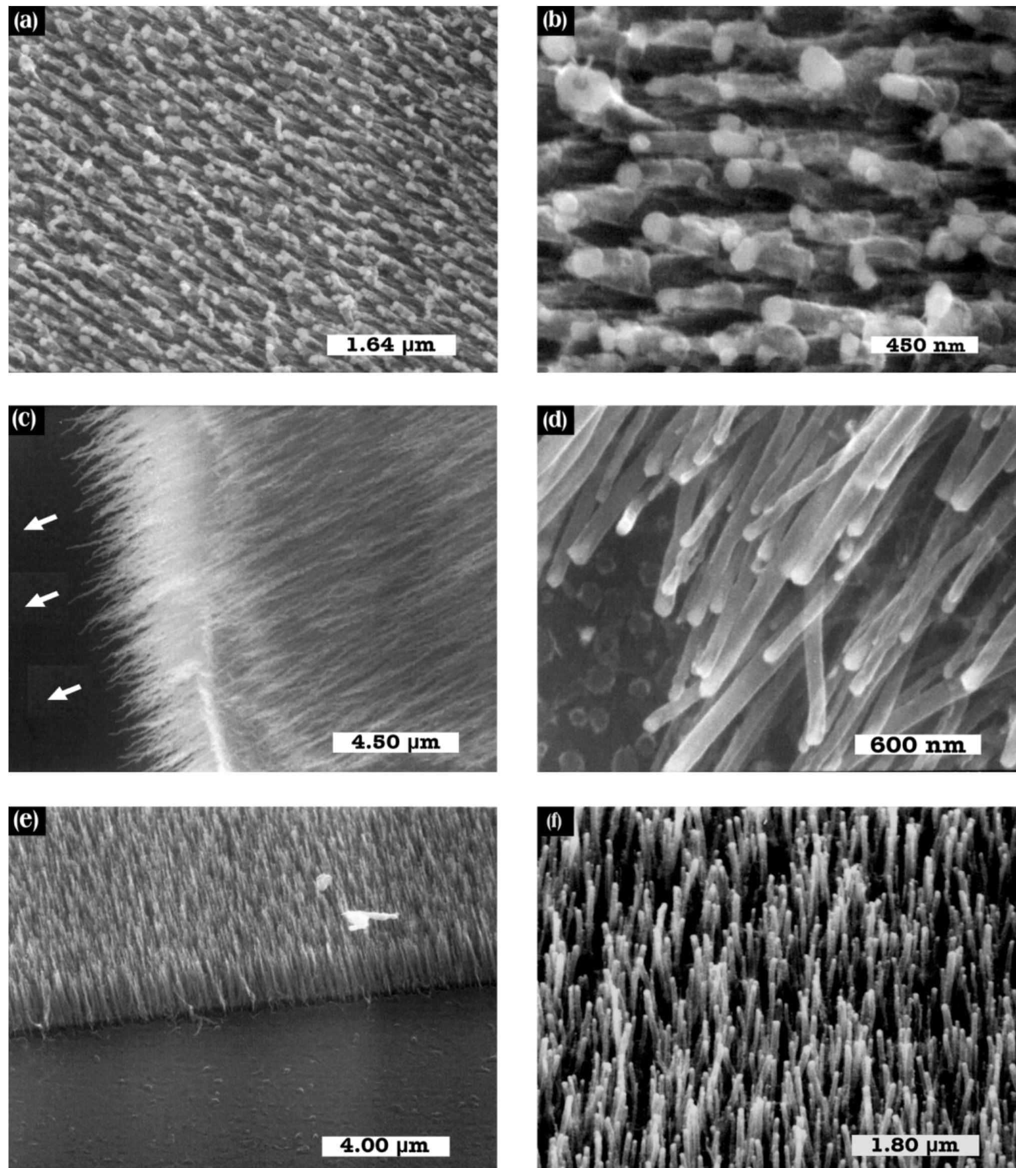

Fig. 1. SEM morphologies of CNTs under three different deposition conditions: (a) and (b) the guided flow and 5 min deposition time (Sample A); (c) and (d) the guided flow and 15 min deposition time (Sample B); (e) and (f) the unguided flow and 15 min deposition time (Sample C), where Figs. (b), (d) and (f) are at higher magnifications.

grown by the un-guided flow for 15 min is called Sample C.

The morphologies, microstructures and bonding structures of the deposited CNTs were characterized by field emission scanning electron microscopy, transmission electron microscopy (TEM) and Raman spectroscopy, respectively. The field emission properties were determined by current density versus electric field (J–E) measurements under vacuum and electrode distance 100 μm. The anode is 2 mm in diameter. The electrode distance was defined by the electrode–substrate–surface distance plus the average CNTs film thickness.

3. Results and discussion

3.1. Effect of the guided flow under negative bias on the growth direction of CNTs

The SEM morphologies of the CNTs are shown in Fig. 1a and b for Sample A, Fig. 1c and d for Sample B, Fig. 1e and f for Sample C. Fig. 1b, d and f are at higher magnifications than the corresponding Fig. 1a, c and e. Where the Samples A and B are grown under the guided flow (inserting Ti wafer on the top of specimen) for 5 and 15 min deposition times, respec-

tively. In contrast, the Sample C is grown under the unguided flow (no Ti wafer above the specimen) for 15 min deposition time. In addition, Fig. 1b, e and f are about the 45°-titled micrographs, and Fig. 1a, c and d are top view micrographs. It is quite obvious that the CNTs in the top view of Fig. 1c are horizontally oriented, where the CNTs were grown beyond the substrate edge boundary, as indicated by the arrows showing the CNTs growth direction. Accordingly, the aligned CNTs in Fig. 1a–d are nearly parallel to the substrate surface with the bending angles approximately 6–8°. In contrast, the aligned CNTs shown in Fig. 1e and f are almost perpendicular to the substrate surface. By comparing the average diameters and lengths of the CNTs in Fig. 1a–d, it indicates that there are no significant difference in average tube diameter for deposition times of 5 and 15 min (Samples A and B, respectively), but the average tube length of Sample B (~3 μm) is more than eight times of Sample A (~350 nm). This signifies that the growth rate is an increasing function of deposition time. By comparing the length of CNTs in Fig. 1c (~3 μm) and e (~2 μm) at the same deposition time, the growth rate of the CNTs for the guided flow is relatively higher than for the unguided flow.

The TEM micrograph of CNTs for the guided flow (Sample B) is shown in Fig. 2. The inset is the electron diffraction pattern of CNTs with Co catalyst on the free surface end of the tube, indicating the diffraction spots of Co catalyst and the (0 0 2) diffraction rings of CNT. It is noted that the growth can be assigned to the tip-growth mechanism [22,29,30], as indicated by the embedded Co particles at the tips of CNTs, which were shown in Fig. 1a–d. Similar phenomena are observed for the CNTs grown by the unguided flow. This is in agreement with the previous results where the Co catalysts were applied by different methods [29].

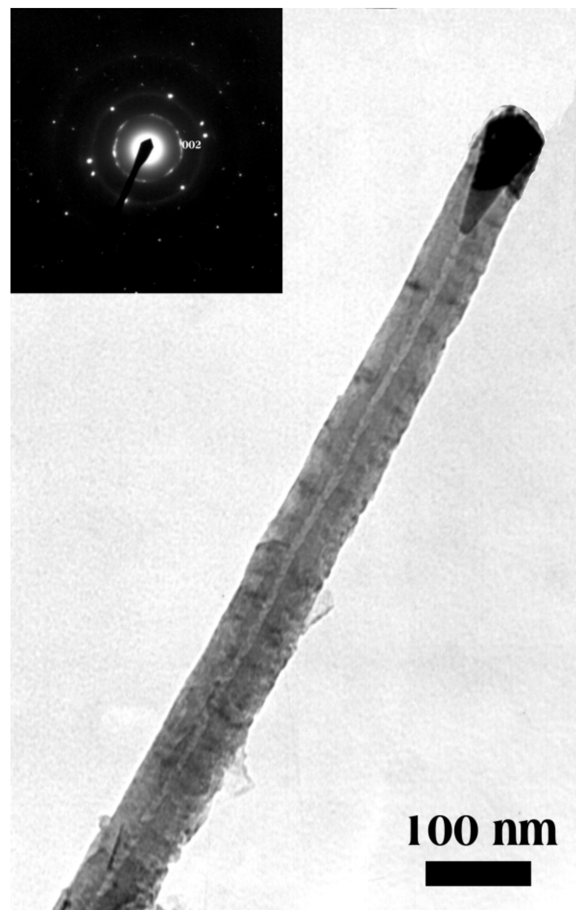

Fig. 2. TEM micrographs of the CNTs under the guide flow and 15 min deposition time (Sample B), where the inset is electron diffraction pattern at the catalyst-embedded CNTs tips.

3.2. Growth mechanism of the horizontally-aligned CNTs

The growth mechanisms of the aligned CNTs have been an open question since its discovery. The growth of vertically-aligned CNTs were reported in various different catalysts-assisted deposition methods, such as CVD on mesoporous silica [22], plasma-enhanced CVD on glass substrate [23] and ECR-CVD on Si wafer in our laboratory [29]. The proposed mechanisms are mainly attributed to the effects of DC bias, magnetic field of ECR conditions and/or self-bias of plasma [29–31]. On the other hand, the horizontally-aligned CNTs have been prepared by thermal CVD on patterned Si towers [32] and by the electric field-assisted thermal CVD [33]. The growth mechanisms of these CNTs bridges are still a controversy issue. The proposed mechanisms are based on the following arguments: growth competition due to interaction between flow rate and flow direction differences plus van der Waals interaction [30,31]; growth directed by interaction between electric field and the CNTs [32], where the field-alignment effect originates from the high polarizability of CNTs. In the present work, the source gases were guided to flow horizontally relative to the substrate surface, and a negative DC bias (−200 V) was applied to the substrate. We propose that the guided flow would restrict the growth in vertical direction, and the electric potential difference between the substrate and chamber wall would guide the ions to flow toward the chamber wall, and so would bend the CNTs horizontally. This is in agreement with the experimental results shown in Fig. 1c, where the horizontally-aligned CNTs are self-sustained beyond the substrate edge boundary toward the chamber wall.

3.3. Raman spectra and field emission properties

With 2 μm of the laser spot size, Fig. 3 depicts the micro-Raman spectra of the vertical and horizontal CNTs

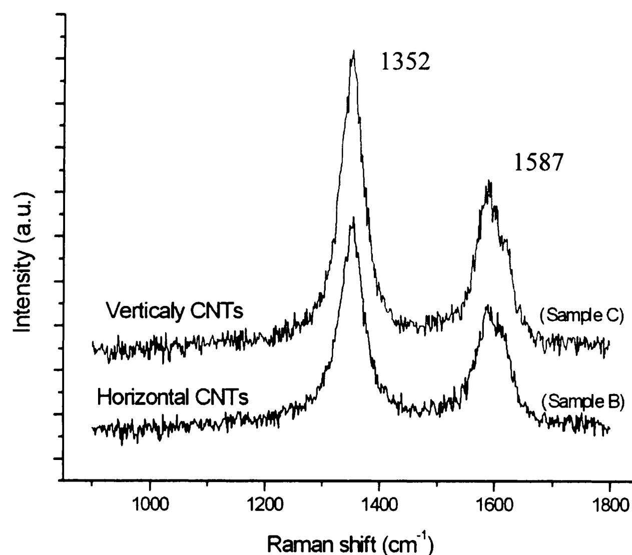

Fig. 3. Typical Raman spectra of the vertical and horizontal CNTs (Samples B and C).

for Samples B and C, respectively. The D-line (sp^3 bonding) at 1353/cm corresponds to the defect types on the graphene layers, such as dislocations, pentagonal and heptagonal lattices; and G-line (sp^2 bonding) at 1587/cm corresponds to the crystalline graphene sheets. By examining the I(G)/I(D) ratio, the ratios for vertical and horizontal CNTs are 0.68 and 0.52, respectively. It is understandable that the Raman signals of vertical CNTs can not completely represent the defect structures of the whole CNTs due to the blocking effect of the catalysts at the tips and the limitation of laser penetration, and therefore the Raman signals of the vertical CNTs represent the defect structures around the tip area only. In contrast, the Raman signals of the horizontally-aligned CNTs are from the body of the CNTs, and so represent the bonding nature of the whole CNTs. In other words, the I(G)/I(D) ratio of 0.68 for the vertical CNTs can not represent its true defect density.

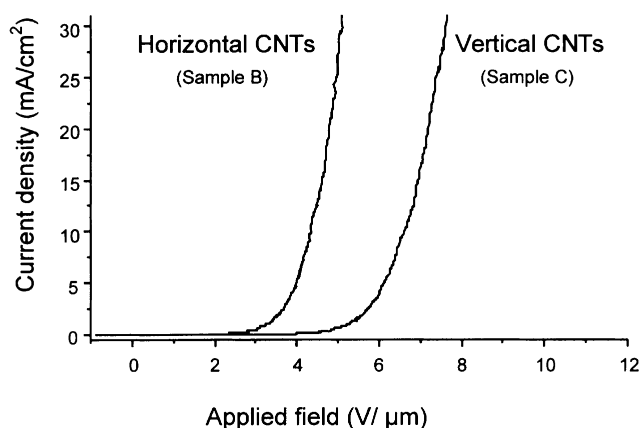

Fig. 4. Typical field emission J–E curves of the vertical and horizontal CNTs (Samples B and C).

Fig. 4 illustrates the J–E curves of the vertical and horizontal CNTs for Samples B and C, by measuring at the same electrode distance 100 μm. It is obvious that the horizontal CNTs show better field emission properties, i.e. for horizontal CNTs, turn-on electric field ($E_{\text{turn-on}}$)=2 V/μm (at J=1 μA/cm^2), threshold electric field (E_{th})=4.3 V/μm (at J=10 mA/cm^2); for vertical CNTs, $E_{\text{turn-on}}$=3 V/μm, E_{th}=6.6 V/μm. This may be due to the fact that the field emission of the vertical CNTs is more restricted by the catalysts at the tips and their effective emission area from defects of the CNTs body is effectively diminished by the neighbor CNTs, in contrast to field emission from the body instead of tips for the horizontal CNTs. This is in agreement with the results of a related work, where the CNTs were grown or rolled into different orientations to compare the field emission properties [34].

4. Conclusions

Large-area well-aligned CNTs with vertical and horizontal orientations could be obtained by manipulating the gas flow direction and the electric field on the deposition substrate. This novel process permits to synthesize horizontally-aligned CNTs, which is a very promising way to apply CNTs in microelectronic devices in the future. The possible growth mechanism of horizontal CNTs is proposed. The field emission properties can be manipulated by changing the orientation of CNTs.

Acknowledgments

The authors would like to thank the supports of the National Science Council (Contract No.: NSC90-2216-E-009-034, -035 and -040) and the Ministry of Education of Taiwan (Contract No.: 89-E-FA06-1-4).

References

[1] H. Dai, E.W. Wong, C.M. Lieber, Science 272 (1996) 523.
[2] P.G. Collins, A. Zettl, H. Bando, A. Thess, R.E. Smalley, Science 278 (1997) 100.
[3] R. Martel, T. Schmidt, H.R. Shea, T. Hertel, P.H. Avouris, Appl. Phys. Lett. 73 (1998) 2447.
[4] L. Roschier, J. Penttila, M. Martin, P. Hskonen, M. Paalanen, U. Tapper, E.I. Kauppinen, C. Journet, P. Bernier, Appl. Phys. Lett. 75 (1999) 728.
[5] M. Antonietti, B. Berton, C. Göltner, H.P. Hentze, Adv. Mater. 10 (1998) 154.
[6] B.T. Holland, C.F. Blanford, A. Stein, Science 281 (1998) 538.
[7] J.E.G.J. Wijnhoven, W.L. Vos, Science 281 (1998) 802.
[8] P. Yang, T. Deng, D. Zhao, P. Feng, D. Pine, B.F. Chmelka, G.M. Whitesides, G.D. Stucky, Science 282 (1998) 2244.
[9] A.G. Rinzler, J.H. Hafner, P. Nikolaev, L. Lou, S.G. Kim, D. Tomanek, P. Nordlander, D.T. Cobert, R.E. Smalley, Science 269 (1995) 1550.

[10] W.A. de Heer, A. Chatelain, D. Ugarrte, Science 270 (1995) 1179.
[11] Q.H. Wang, A.A. Setlur, J.M. Lauerhaas, J.Y. Dai, E.W. Seelig, Appl. Phys. Lett. 72 (1998) 2912.
[12] P.G. Collins, A. Zettl, Appl. Phys. Lett. 69 (1996) 1969.
[13] Q.H. Wang, T.D. Corrigan, J.Y. Dai, R.P.H. Chang, Appl. Phys. Lett. 70 (1997) 3308.
[14] C. Journet, W.K. Maser, P. Bernier, A. Loiseau, M. Lamy, de la Chapelle, S. Lefrant, P. Deniered, R. Lee, J.E. Ficher, Nature 388 (1997) 756.
[15] A.C. Dillon, K.M. Jones, T.A. Bekkedahl, C.H. Kiang, D.S. Bethune, M.J. Heben, Nature 386 (1997) 377.
[16] H. Dai, J.H. Hafner, A.G. Rinzler, D.T. Rinzler, D.T. Colbert, R.E. Smalley, Nature 384 (1996) 147.
[17] G. Che, B.B. Lakshmi, E.R. Fisher, C.R. Martin, Nature 393 (1998) 346.
[18] D.S. Bethune, C.H. Klang, M.S. de Vries, G. Gorman, R. Savoy, J. Vazquez, R. Beyers, Nature 363 (1993) 605.
[19] A. Thess, R. Lee, P. Nikolaev, H. Dai, P. Petit, J. Robert, C. Xu, Y.H. Lee, S.G. Kim, A.G. Rinzler, D.T. Colbert, G. Scuseria, D. Tomanek, J.E. Fisher, R.E. Smalley, Science 273 (1996) 483.
[20] L.C. Qin, D. Zhou, A.R. Krauss, D.M. Gruen, Appl. Phys. Lett. 72 (1998) 3437.
[21] C.J. Lee, J. Park, Appl. Phys. Lett. 77 (2000) 3397.
[22] W.Z. Li, S.S. Xie, L.X. Qian, B.H. Chang, B.S. Zou, W.Y. Zhou, R.A. Zhao, G. Wang, Science 274 (1006) 1701.
[23] Z.F. Ren, Z.P. Huang, J.W. Xu, J.H. Wang, P. Bush, M.P. Siegal, P.N. Provencio, Science 282 (1998) 1105.
[24] J. Kong, H.T. Soh, A.M. Cassell, C.F. Quate, H. Dai, Nature 395 (1998) 878.
[25] A.M. Cassell, N.R. Franklin, T.W. Tombler, E.M. Chan, J. Han, H. Dai, J. Am. Chem. Soc. 121 (1999) 7975.
[26] H.T. Soh, C.F. Quate, A.F. Morpurgo, C.M. Marcus, J. Kong, H. Dai, Appl. Phys. Lett. 76 (2000) 627.
[27] C. Zhou, J. Kong, H. Dai, Appl. Phys. Lett. 76 (2000) 1597.
[28] Y.S. Han, J.K. Shih, S.T. Kim, J. Appl. Phys. 90 (2001) 5731.
[29] C.H. Lin, H.L. Chang, M.H. Tsai, C.T. Kuo, Diam Relat Mater, in press.
[30] C. Bower, W. Zhu, S. Jin, O. Zhou, Appl. Phys. Lett. 77 (2000) 830.
[31] S.H. Tsai, C.W. Chao, C.L. Lee, H.C. Shih, Appl. Phys. Lett. 74 (1999) 3462.
[32] N.R. Franklin, H. Dai, Adv. Mater. 12 (2000) 890.
[33] Y. Zhang, A. Chang, J. Cao, Q. Wang, W. Kim, Y. Li, N. Morris, E. Yenilmez, J. Kong, H. Dai, Appl. Phys. Lett. 79 (2001) 3155.
[34] Y. Chen, D.T. Shaw, L. Guo, Appl. Phys. Lett. 76 (2000) 2469.